JurnalPolimesin
Department of Mechanical Engineering
State Polytechnic of Lhokseumawe
http://e-jurnal.pnl.ac.id/polimesin
e-ISSN : 2549-1999 No. : 6 Month :December
p-ISSN : 1693-5462 Volume : 21 Year : 2023

Article Processing Dates: Received on 2023-08-28, Reviewed on 2023-09-06, Revised on 2023-10-22, Accepted on 2023-11-15 and Available online on 2023-12-30

Performance investigation of installed pico-hydro power using maximum power point tracking based on incremental conductance algorithm in solar water pumped storage system

Novan Akhiriyanto*, Wasis Waskito A, Akbar Pratama, Radith Satria P
Teknik Instrumentasi Kilang, Politeknik Energi dan Mineral Akamigas, Blora, 58315, Indonesia
*Corresponding author: akhiriyanto.n@gmail.com

Abstract

The Solar Water Pumped Storage System (SWPS) has been gaining popularity as an environmentally friendly and sustainable solution to address water supply challenges in areas with abundant solar radiation. The potential energy stored in SWPS is harnessed by converting it into electrical energy through the installed pico-hydropower (picoHP) within the SWPS distribution pipe system. PicoHP performance depended on the flow rate and water pressure, which could not be naturally controlled, leading to low reliability in picoHP generation. This research aimed to optimize picoHP performance through engineering changes in pipe diameter and voltage regulation using a SEPIC MPPT circuit based on the Incremental Conductance (INC) algorithm. The parameters affecting the voltage and current of the picoHP were the water level in the tank and the choice of pipe adapter type based on changes in pipe diameter. The SEPIC MPPT circuit with the INC algorithm began operating when the input voltage from the picoHP reached 7.56 V, resulting in an output voltage of 11.2 V with a duty cycle (D) 25%. This indicated a delay in the operation of the SEPIC MPPT with the INC algorithm due to the computational process, which did not respond quickly when the input voltage from the picoHP started to decrease. The electrical energy generated by the picoHP through the SEPIC MPPT circuit successfully charged the battery through the BMS module.

Keywords:
PicoHP, MPPT, INC algorithm, pipe adapter, SEPIC MPPT, duty cycle, BMS.

1 Introduction

The Solar Water Pumping System (SWPS) has been extensively employed in self-reliant rural areas to provide independent electrical energy for operating water pumps in agricultural wells for irrigation purposes [1][2]. The proposed pump type in our study utilizes a DC pump because in its application, it produces a higher water output than an AC pump, based on [3]. Another advantage is that operating a DC pump does not require power conversion devices since the electrical energy generated by PV solar generation is in a DC system [4]. As its name implies, the water pump utilizes the electrical energy generated by PV panels. However, PV panel technology is still in the research phase, with current efficiencies reaching up to 27.6% [5]. Commercially available PV panels generally exhibit lower efficiencies than this value. Conversely, the water pumped storage technique has been widely adopted to harness the potential energy stored in tanks or water reservoirs [2].

The opportunity to install pico-hydropower (picoHP) in SWPS appears to be promising [6]. However, experimentally, SWPS needs to generate a minimum flow rate of 5.8 L/min to enable picoHP to operate at a nominal DC voltage of 12 V with a power of 0.602 W and up to 1.121 W at a flow rate of 8.9 L/min. This experiment was conducted by mounting the picoHP on the household water pipe[7].

Studies on picoHP as a secondary electrical energy source are rarely conducted. The picoHP studies that have been carried out focus on the design and control of a solar-based UPS to regulate the picoHP alternator's excitation in the microgrid system. In other words, the electrical energy generated by the solar power system serves as a backup for the picoHP's excitation voltage to mitigate the harmonics arising from picoHP generation itself [8]. Although there have been studies on picoHP as the primary generator in rural communities, these picoHP systems are based on AC, requiring additional converter devices to address turbine speed variations and consumer load fluctuations, leading to voltage and frequency fluctuations. Therefore, the purpose of this study is to review voltage and frequency control technology [9].

Our study proposes the integration of PV solar generation as the primary source of electrical energy for powering a DC 12V 180W pump load. To harness the potential energy obtained from the gravitational flow of water resulting from the water height stored in a tank under certain conditions, our research proposes a combination of SWPS and adding picoHP devices installation with a capacity of 10 Watts per unit. It is expected that this combination will be able to harvest the potential energy along the water flow from the tank outlet, which will be converted into electrical energy and stored in batteries through a Battery Management System (BMS) device. The proposed picoHP device has specifications to generate a DC voltage of 12 Volt. However, in the SWPS system, it is necessary to minimize head loss along the pipeline to maintain optimal performance, as in [10]. Therefore, the proposed scheme utilizes PolyVinyl Chloride (PVC) pipes, known for their low surface roughness and easy accessibility in the market. Additionally, engineering modifications are implemented to adjust the flow pipe to achieve optimal water pressure and flow rate by varying the pipe diameter as in [11][12].

Moreover, to allow the nominal DC voltage of 12 V of the picoHP device to deliver electrical energy to the battery through the BMS with a DC nominal voltage charging of 14.4 to 15 VDC, the operational voltage of the picoHP device needs to be adjusted to minimum 14.4 VDC. This can be achieved by employing a Maximum Power Point Tracking (MPPT) mechanism referred to [13] in the form of a Single Ended Primary Inductance Converter (SEPIC) circuit, which can step up or step down the DC output voltage with the same polarity referred to [14].

2 ResearchMethods

The proposed system design model, as shown in Fig. 1 below, comprises solar panels that convert solar irradiance into electrical energy. This electrical energy is subsequently stored in batteries using a Solar Charge Controller (SCC). The stored energy powers a DC pump, which draws water from a well and transfers it to a water tank. The potential energy of the stored water in the tank is then harnessed to generate electrical energy through a picoHP. Each picoHP unit is currently capable of producing a maximum of 10 W of electrical energy. Three picoHP units are installed with a tee pipe connection to enhance the likelihood of electrical energy generation. This electrical energy is stored in small-capacity batteries through a BMS module, with DC voltage control provided by the SEPIC MPPT circuit. These small-capacity batteries are used to supply electrical energy to the load of small lighting and controllers.

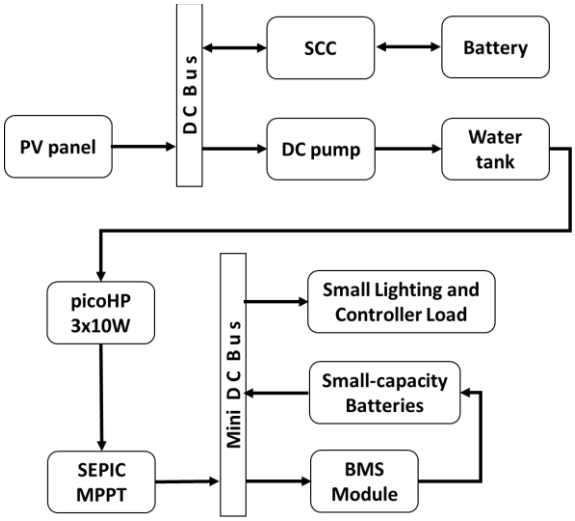

Fig. 1. Proposed system design model.

This study was conducted experimentally using a prototype design that was implemented in the field. The selection of solar module capacity is determined by the main load in the system. The most dominant load in this system is a 180 W DC pump with a voltage of 12 V. The capacity of the PV panel is 250 Wp with a maximum voltage of 30.3 V, and the open circuit voltage of 36.3 V with a maximum current is 8.25 A, and short circuit current is 8.75 A. PV panel connected by SCC of 20 A and battery 12 V 70 Ah.

A 3.2-meter tower is used to support the tank with a volume of 1050 L and other components mentioned above. The protection and control equipment is housed inside an electrical panel box, which is also suspended on the tower below the tank. Three units of picoHP are installed, as shown in Fig. 2, in a piping system with engineered changes in pipe diameter, or what we refer to as a pipe adapter with specifications of ¾ inch to 2 inches and then back to ¾ inch, as the entire piping system uses a ¾ inch diameter.

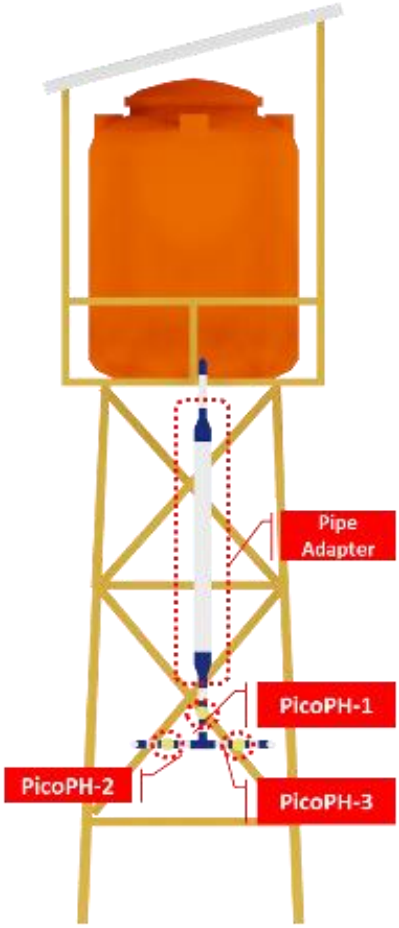

Fig. 2. Prototype SWPS design.

The purpose of installing the pipe adapter is to minimize pressure losses in the flow of water through the pipe when the outlet valve is turned on. In the piping system, sensors are also installed. Flow rate sensors are installed to measure the flow rate of water passing through the picoHP device [15]. Pressure sensors are used to measure the pressure at the inlet and outlet sides of the picoHP device. By obtaining the values of flow rate and pressure, the performance of the picoHP device can be analyzed. Additionally, voltage and current sensors are installed in the panel box to measure the voltage and current from the picoHP device, enabling the determination of the power generated by the picoHP.

2.1 SEPIC MPPT Circuit

MPPT is a device used to search for the maximum power point, utilizing a DC/DC converter circuit connected to the output energy from the picoHP system. The DC/DC converter circuit used in this MPPT is a SEPIC, which can increase and decrease its output voltage using non-polarity reversing switching with high precision. The mathematical equation for calculating the components in the SEPIC as shown in Eq. 1 - Eq. 5[16].

$$\frac{V_o}{V_s} = \frac{D}{1-D} \tag{1}$$

$$L_1 = \frac{V_s D}{\Delta I_{L1} f} \tag{2}$$

$$\boldsymbol{C_1 = \frac{V_o D}{\Delta V_{C1} f}} \tag{3}$$

$$L_2 = \frac{V_s D}{\Delta I_{L2} f} \tag{4}$$

$$C_2 = \frac{V_o D}{\Delta V_{C2} f} \tag{5}$$

where*Vo* is the output voltage, *Vs* is the supply/input voltage, *D* is the duty cycle, *L* is the inductor, *C* is the capacitor, and *f* is the switching frequency.

SEPIC circuit prototype consists of 2 inductors 100µH, 2 capacitors 100µF, a transistor IRF540N, and a diode 1N5392. The prototype of the SEPIC circuit that has been constructed is shown in Fig. 3.

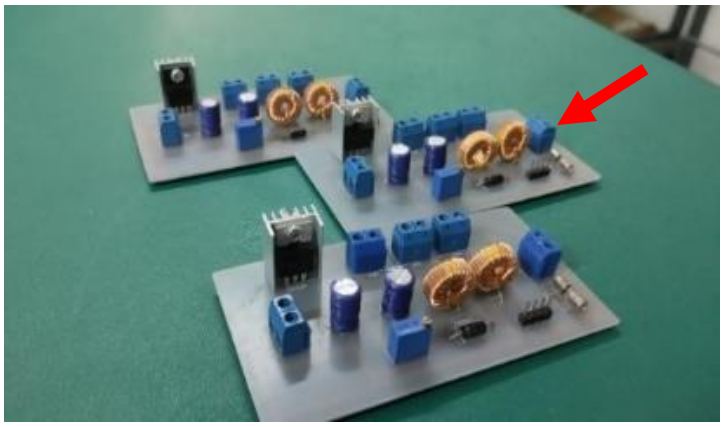
Fig. 3. SEPIC prototype.

The installation of the SEPIC MPPT circuit is used to convert the output voltage from 3 picoHP units. The output voltage of the picoHP is obtained from the voltage and DC power sensor INA219. Then, the INA219 sensor sends this voltage data to the microcontroller to adjust the duty cycle (*D*) in the SEPIC MPPT circuit toachieve the desired output voltage following the voltage specification of the BMS used for charging the LiFePO4 batteries [17]. The installation diagram of the SEPIC MPPT circuit in the SWPS system can be seen in Fig. 4.

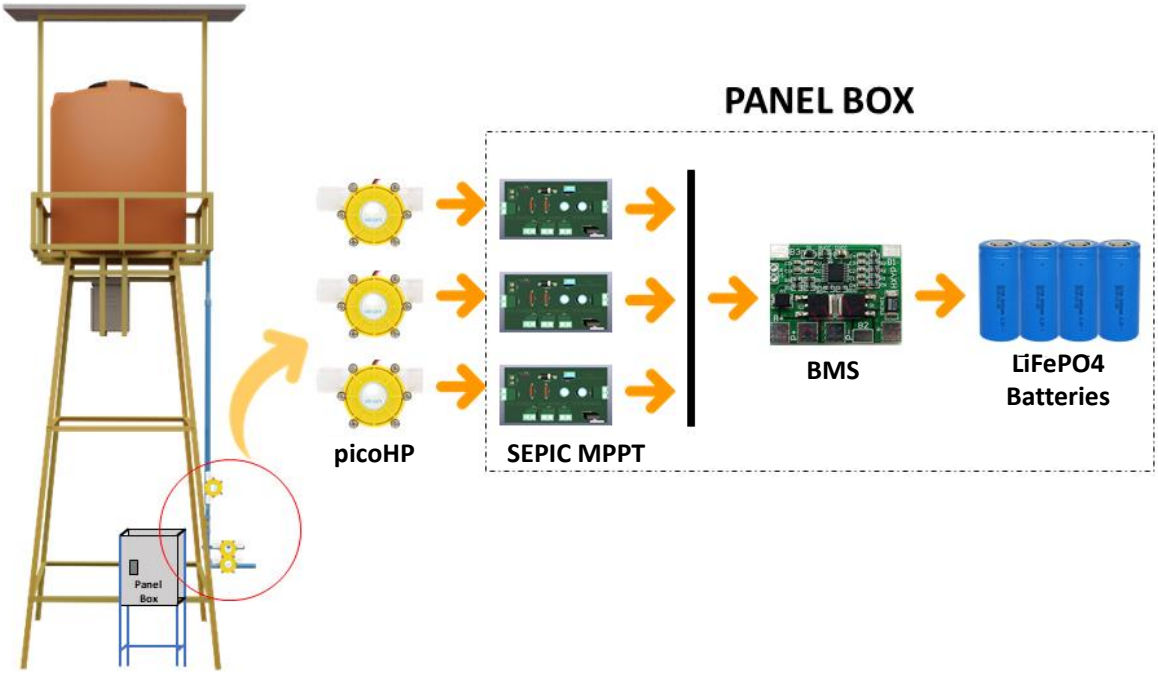

Fig. 4. SEPIC MPPT installation in SWPS.

BMS is an electronic circuit module designed to oversee the operation of batteries. Its main functions are to regulate battery performance, safeguard battery cells, control battery temperature, balance cell charging, and manage battery charging and discharging processes. The BMS module used in this study is shown in Fig. 5.

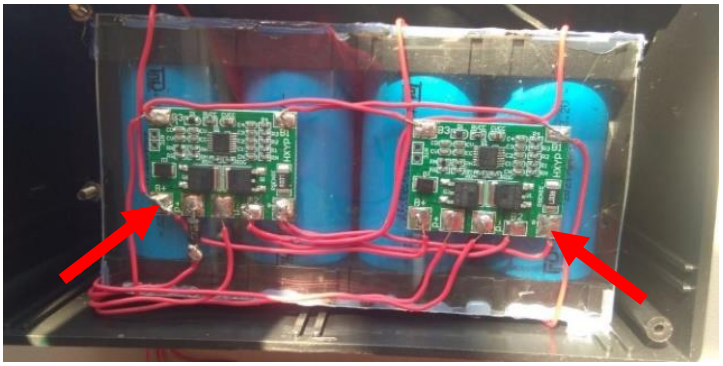

Fig. 5. BMS LiFePO4 4S module with batteries.

The BMS constantly monitors the real-time voltage and current values of the battery, and energy charging and usage occur exclusively through the same bus terminals. Utilizing a BMS offers several advantages, including preventing overcharging and over-discharging to maximize battery lifespan, protecting against short circuits, ensuring balanced charging and discharging of individual battery cells, monitoring battery temperature for optimal performance, and providing real-time calculations of the stored charge within the battery. The specification of the BMS module used in this study is shown in Table 1.

Table 1. Specification of BMS module

Specification	Description
BMS	BMS $LiFePO_4$ 4S
Nominal current	8A
Maximum current	20A
Charging voltage	14.4VDC ~ 15VDC

2.2 Incremental Conductance (INC) Algorithm

Incremental Conductance(INC) algorithm is commonly used due to its high accuracy in tracking the steady state and its ability to adapt well to rapid changes in weather conditions [18]. This algorithm operates on the principle that the slope of the P-V characteristic of the PV module is zero at the Maximum Power Point (MPP), negative to the right of the MPP, and positive to the left. Thus, the relationship can be expressed as Eq. 6[16].

$$\frac{dP}{dV} = I + V\frac{dI}{dV} \cong I + V\frac{\Delta I}{\Delta V} \quad (6)$$

The MPP is determined by comparing the instantaneous conductance $\left(\frac{I}{V}\right)$ with the incremental conductance $\left(\frac{\Delta I}{\Delta V}\right)$. The flowchart of INC algorithm can be seen in Fig. 6.

This algorithm will evaluate the condition of the difference or variance in conductance values $\left(\frac{\Delta I}{\Delta V}\right)$ in each iteration in order to obtain a value of $\frac{\Delta I}{\Delta V} = -\frac{I}{V}$. If the conductance values are not equal, the difference should be added or subtracted to achieve the condition of $\frac{\Delta I}{\Delta V} = -\frac{I}{V}$.

INC algorithm is written in MicroPython programming language and then uploaded to the ESP32 microcontroller module along with the code for current, voltage, and power sensors. The ESP32 controls the duty cycle (D) as the switching of the IRF540N MOSFET in the SEPIC circuit at a frequency of 100 kHz and also the INA 219 sensor with a 0.5 second reading delay [19].

3 Results and Discussion

This research utilizes three scenarios of pipe adapters, which are: 1) without changing the pipe diameter, the overall diameter of ¾ inch is referred to as PA-1; 2) with a change in pipe diameter from ¾ inch to 1½ inch and then back to ¾ inch, it is referred to as PA-2; 3) with a change in pipe diameter from ¾ inch to 2 inches and then back to ¾ inch, it is referred to as PA-3.

The measurement results using flow sensor on piping installation and voltage sensors on 3 picoHP units installed according to Fig. 2 are displayed in the following Table 2.From Table 2, the pipe adapter PA-3 is considered more suitable for implementation compared to PA-1 and PA-2. This is because, inall water level conditions in tank H, the 3picoHP units with PA-3 show larger measurement results compared to the others in all H conditions. This can be observed from the higher flow rate Q in all H conditions, as Q affects the rotational speed of the picoHP blades to generate voltage in no-loadconditions.

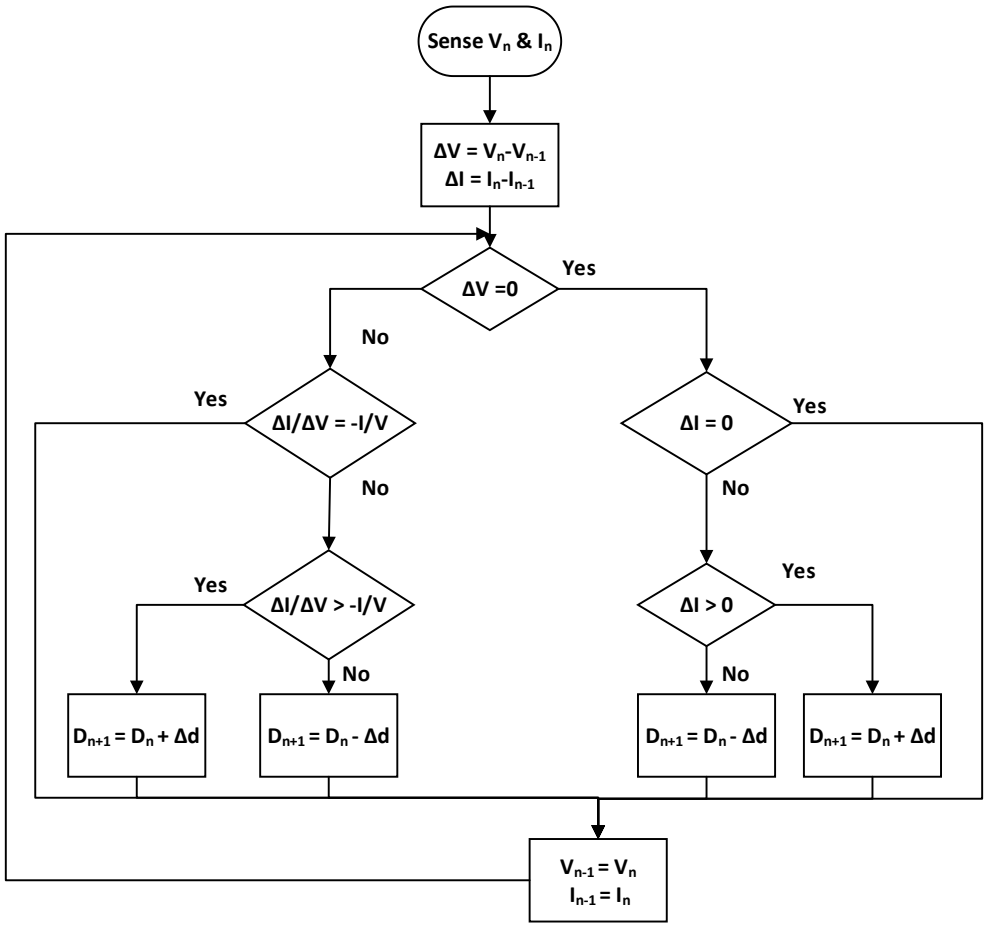

Fig. 6. INC algorithm flowchart.

Table 2. Measured voltage of picoHP

Type of pipe adapter	H (cm)	Q (L/m)	picoPH-1 (V)	picoPH-2 (V)	picoPH-3 (V)
PA-1	110	5.88	12.01	5.9	6.11
PA-2	110	5.95	12.03	5.88	6.2
PA-3	110	6.01	12.04	6.22	6.28
PA-1	70	5.52	11.87	5.41	5.45
PA-2	70	5.6	11.97	5.48	5.52
PA-3	70	5.72	11.98	5.56	5.6
PA-1	30	5.18	11.75	4.65	4.72
PA-2	30	5.22	11.88	4.67	4.8
PA-3	30	5.28	11.9	4.88	4.9

Although the increase in water flow rate in all tank water level conditions is not significant, PA-3 is chosen to be installed in this system. This is because, at the minimum tank water level condition of 30 cm, the voltage generated by picoHP-2 and picoHP-3 is still higher, approaching 5 V, compared to if PA-1 and PA-2 were installed, where the voltages for picoHP-2 and picoHP-3 are 4.88 V and 4.9 V, respectively. Additionally, at the 30 cm tank water level, PA-3 also provides results that are closest to 12 V for the voltage generated by picoHP-1, which is 11.9 V.

To optimize their performance, especially for picoHP-2 and picoHP-3, a SEPIC converter circuit needs to be installed as an MPPT with an INC algorithm by adjusting the duty cycle (*D*) to maintain the voltage, following the voltage specification of the BMS used.

From Table 2, picoHP-1 generates a voltage of approximately 12 V, while picoHP-2 and picoHP-3 generate a voltage of around 5V in the no-load test. As shown in Fig. 1, picoHP-1 is installed after the output of the pipe adapter, while picoHP-2 and picoHP-3 are installed after the tee branch. Therefore, the flow rate of water passing through picoHP-1 can flow smoothly after experiencing minimal pressure loss, while the flow rate of water passing through picoHP-2 and picoHP-3 experiences turbulent velocity distribution and water hammer due to the branching. This can reduce the voltage generated by picoHP-2 and picoHP-3.

From the measurement data obtained in Table 2, the SEPIC MPPT circuit without the INC algorithm was tested using a power supply module as the input voltage source to the SEPIC MPPT circuit with a duty cycle (*D*) increment of 1% to obtain the desired output voltage according to the BMS specifications. Fig. 7 shows the input voltage graph of 5 V using the power supply module with a 1% increment in *D* and the input power, resulting in the output voltage and power of the SEPIC MPPT circuit.

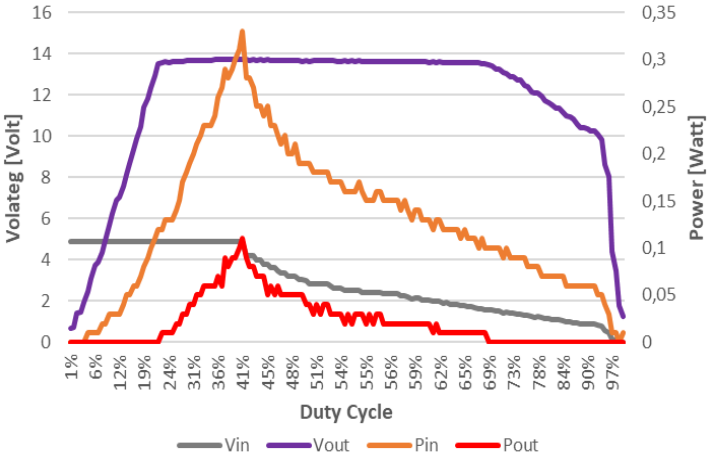

Fig. 7. Test of SEPIC MPPT output connected to BMS at voltage input 5 V.

From Fig. 7, it can be observed that the output current starts to flow at *D* = 24% with an output voltage of 13.55V at an input voltage of 4.9V, while the maximum output power of 0.1W is obtained at *D* = 40% with an output voltage of 13.72 V at an input voltage of 4.88V. As for the 12 V input voltage, it can be seen in Fig. 8.

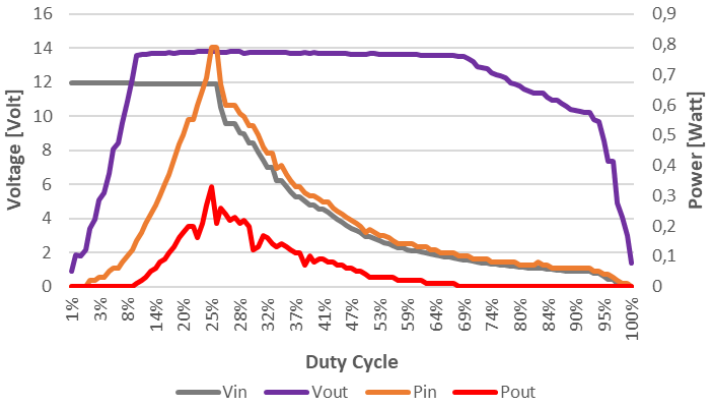

Fig. 8. Test of SEPIC MPPT output connected to BMS at voltage input 12 V.

From Fig. 8, it can be observed that the output current starts to flow at D = 10% with an output voltage of 13.58 V at an input voltage of 11.92 V, while the maximum output power of 0.33 W is obtained at D = 25% with an output voltage of 13.8 V at an input voltage of 11.91 V.

If previously there was a test of the SEPIC MPPT circuit output connected to the BMS but the input voltage source was obtained through a power supply module, the following test was conducted with no load and without being connected to the BMS. The picoHP was used as the input voltage supply, and the output voltage obtained is shown in Fig. 9.

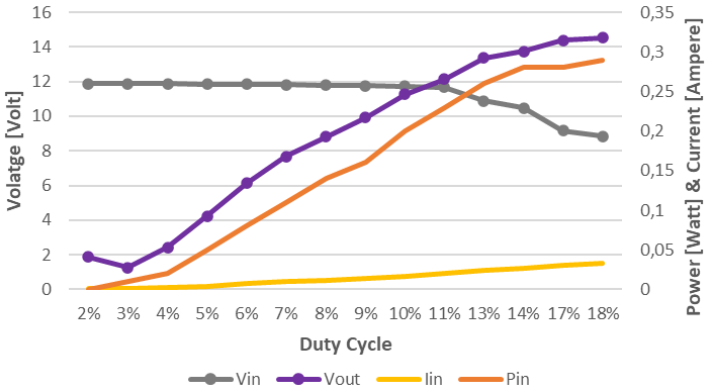

Fig. 9. No load test of SEPIC MPPT voltage output with picoHP as input voltage supply.

The data obtained in Fig. 9 is from testing with a 1% increment in D without using the INC algorithm. It was found that at D = 11% with the input voltage from the picoHP, the output voltage can reach 12.14 V. To obtain an output voltage higher than 13.5 V for connection to the BMS, at D = 14% with an input voltage from the picoHP of 10.49 V, the output voltage of the SEPIC MPPT circuit reaches 13.73 V.

As for the output voltage in the no-load test, when the SEPIC MPPT circuit with the INC algorithm is used, it can be seen in Fig. 10 that the SEPIC MPPT circuit with the INC algorithm is more sensitive in handling changes in the input voltage supplied by the picoHP. It is noted that at an input voltage of 11.97 V, the SEPIC MPPT circuit with the INC algorithm can sensitively increase the output voltage to 13.38 V at D = 10%. However, the output voltage of 13.38 V is not sufficient to supply current to the BMS, so the output voltage needs to be increased to more than 13.5 V. Therefore, the duty cycle needs to be further increased to D = 11%, resulting in an output voltage of 13.56 V.

The specification of the BMS states that the input voltage for charging the LiFePO4 battery should be between 14.4 V to 15 V. However, based on the experiments represented in Fig. 7 and Fig. 8, it is observed that the BMS begins charging the LiFePO4 battery at voltages above 13.5 V.

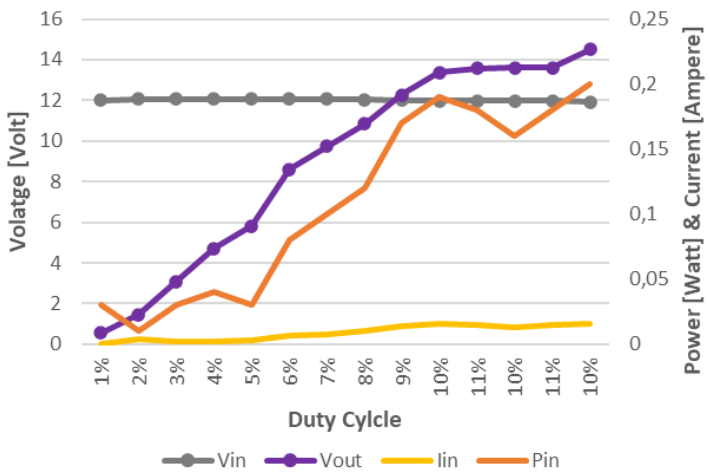

Fig. 10. No load test of INC SEPIC MPPT voltage output with picoHP as input voltage supply.

When the experiment is conducted using the picoHP to charge the battery through the BMS, it is noted that at an output voltage of 11.2 V from the SEPIC MPPT circuit, the current starts flowing to the BMS, resulting in an output power of 3 mW, as seen in Fig. 11.

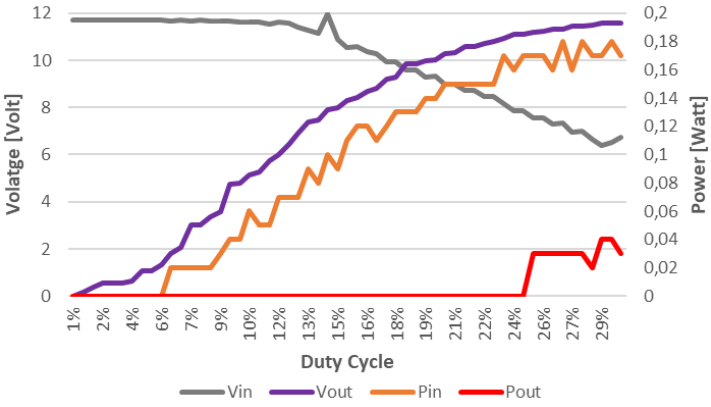

Fig. 11. Test of SEPIC MPPT output connected to BMS at voltage input from picoHP 12V.

The SEPIC MPPT circuit with the INC algorithm starts operating when the input voltage from the picoHP reaches 7.56 V, resulting in an output voltage of 11.2 V at D = 25%. This indicates a delay in the operation of the SEPIC MPPT with the INC algorithm due to the computational process of the algorithm, which may not respond quickly when the input voltage from the picoHP starts to decrease. Ideally, the SEPIC MPPT circuit should start operating when the input voltage from the picoHP drops below 13.5 V, as observed in the experiments shown in Fig. 7 and Fig. 8.

4 Conclusion

In summary, the key parameters affecting the picoHP's voltage, current, and power include water tank level, pipe adapter selection based on pipe diameter changes, and picoHP installation location in the piping system.

The experiments with different voltage sources, including a power supply module and the picoHP, highlighted the SEPIC MPPT circuit's performance. When powered by a power supply module, the circuit effectively achieved the desired output voltage for the BMS module, starting battery charging at 13.5 V. On the other hand, when the picoHP served as the input voltage source with the INC algorithm, it showed a quicker voltage response, surpassing 13.5 V. However, this came at the expense of lower delivered current and reduced output power for battery charging. The use of the INC algorithm improved the SEPIC MPPT circuit's

responsiveness to input voltage changes from the picoHP, particularly in open-circuit conditions. Nevertheless, when the picoHP was the voltage source for the SEPIC MPPT circuit connected to the BMS module load, there was a delay in voltage compensation due to fluctuating input voltage and the INA 219 sensor's 0.5 second reading delay, causing the circuit to start operation at a 7.56V drop in input voltage.

References

[1] K. Kusakana, "Using PV with borehole pumped hydro storage systems for small farming activities in South Africa," in *2017 IEEE Innovative Smart Grid Technologies - Asia (ISGT-Asia)*, Auckland: IEEE, Dec. 2017, pp. 1–6. doi: 10.1109/ISGT-Asia.2017.8378384.

[2] S. Senthil Kumar, C. Bibin, K. Akash, K. Aravindan, M. Kishore, and G. Magesh, "Solar powered water pumping systems for irrigation: A comprehensive review on developments and prospects towards a green energy approach," *Mater. Today Proc.*, vol. 33, pp. 303–307, 2020, doi: 10.1016/j.matpr.2020.04.092.

[3] S. Verma*et al.*, "Solar PV powered water pumping system – A review," *Mater. Today Proc.*, vol. 46, pp. 5601–5606, 2021, doi: 10.1016/j.matpr.2020.09.434.

[4] K. B. Nagne and D. H. K. Naidu, "Comparison of DC-DC Buck Boost and SEPIC Converter for Control of Electronically Commutated BLDC Motor," 2018.

[5] B. Smith, M. Woodhouse, K. Horowitz, T. Silverman, J. Zuboy, and R. Margolis, "Photovoltaic (PV) Module Technologies: 2020 Benchmark Costs and Technology Evolution Framework Results," NREL/TP-7A40-78173, 1829459, MainId:32082, Nov. 2021. doi: 10.2172/1829459.

[6] R. Sharma, S. Sharma, and S. Tiwari, "Design optimization of solar PV water pumping system," *Mater. Today Proc.*, vol. 21, pp. 1673–1679, 2020, doi: 10.1016/j.matpr.2019.11.322.

[7] M. Marwani, M. Z. Kadir, and R. E. Putra, "INVESTIGATION PERFORMANCE OF PICO HYDRO WATER PIPE TURBINE," *Indones. J. Eng. Sci.*, vol. 2, no. 3, pp. 051–058, Sep. 2021, doi: 10.51630/ijes.v2i3.27.

[8] R. Sharma, Seema, and B. Singh, "Design and Control of Solar PV-Pico Hydro Based Microgrid," in *2018 IEEE Industry Applications Society Annual Meeting (IAS)*, Portland, OR: IEEE, Sep. 2018, pp. 1–8. doi: 10.1109/IAS.2018.8544704.

[9] B. A. Mhlambi, K. Kusakana, and J. Raath, "Voltage and Frequency Control of Isolated Pico-Hydro System," in *2018 Open Innovations Conference (OI)*, Johanesburg: IEEE, Oct. 2018, pp. 246–250. doi: 10.1109/OI.2018.8535603.

[10] Š. Tkáč, "Hydro power plants, an overview of the current types and technology," *Sel. Sci. Pap. - J. Civ. Eng.*, vol. 13, no. s1, pp. 115–126, Mar. 2018, doi: 10.1515/sspjce-2018-0011.

[11] T. C. Singh, G. R. K. D. Satyaprasad, K. C. Rath, P. S. Rajesh, and A. Kumar, "Solar PV based PSH system Performance evaluation and analysis for runoff river Pico hydro plant," in *2020 IEEE International Symposium on Sustainable Energy, Signal Processing and Cyber Security (iSSSC)*, GunupurOdisha, India: IEEE, Dec. 2020, pp. 1–6. doi: 10.1109/iSSSC50941.2020.9358851.

[12] Y. A. Çengel and J. M. Cimbala, *Fluid mechanics: fundamentals and applications*. in McGraw-Hill series in mechanical engineering. Boston: McGraw-HillHigher Education, 2006.

[13] A. R. Jordehi, "Maximum power point tracking in photovoltaic (PV) systems: A review of different approaches," *Renew. Sustain. Energy Rev.*, vol. 65, pp. 1127–1138, Nov. 2016, doi: 10.1016/j.rser.2016.07.053.

[14] M. Majstorovic, D. Mrsevic, B. Duric, M. Milesevic, Z. Stevic, and Z. V. Despotovic, "Implementation of MPPT Methods with SEPIC Converter," in *2020 19th International Symposium INFOTEH-JAHORINA (INFOTEH)*, East Sarajevo, Bosnia and Herzegovina: IEEE, Mar. 2020, pp. 1–6. doi: 10.1109/INFOTEH48170.2020.9066296.

[15] Z. Husain, M. Z. Abdullah, and Z. Alimuddin, *Basic fluid mechanics and hydraulic machines*. Hyderabad [India]: BS Publications, 2008.

[16] J. L. Seguel, S. I. Seleme, and L. M. F. Morais, "Comparative Study of Buck-Boost, SEPIC, Cuk and Zeta DC-DC Converters Using Different MPPT Methods for Photovoltaic Applications," *Energies*, vol. 15, no. 21, p. 7936, Oct. 2022, doi: 10.3390/en15217936.

[17] Y.-M. Tseng, H.-S.Huang, L.-S.Chen, and J.-T. Tsai, "Characteristic research on lithium iron phosphate battery of power type," *MATEC Web Conf.*, vol. 185, p. 00004, 2018, doi: 10.1051/matecconf/201818500004.

[18] M. L. Devi, M. Chilambarasan, and C. S. Kumar, "Modeling and simulation of incremental conductance MPPT using self lift SEPIC converter," in *2014 International Conference on Circuits, Power and Computing Technologies [ICCPCT-2014]*, Nagercoil, Tamil Nadu, India: IEEE, Mar. 2014, pp. 867–872. doi: 10.1109/ICCPCT.2014.7054888.

[19] A. Patel and H. Tiwari, "Implementation of INC-PIMPPT and its comparison with INC MPPT by direct duty cycle control for solar photovoltaics employing zeta converter," in *2017 International Conference on Information, Communication, Instrumentation and Control (ICICIC)*, Indore: IEEE, Aug. 2017, pp. 1–6. doi: 10.1109/ICOMICON.2017.8279173.